Electronic Supplementary Material (ESI) for Energy & Environmental Science.

Supplementary Information

I_2 vapor-induced degradation of formamidinium lead iodide based perovskite solar cells under heat-light soaking conditions

Fan Fu[1,2*], Stefano Pisoni[2], Quentin Jeangros[1], Jordi Sastre-Pellicer[2], Maciej Kawecki[3,4], Adriana Paracchino[5], Thierry Moser[2], Jérémie Werner[1], Christian Andres[2], Léo Duchêne[6], Peter Fiala[1], Michael Rawlence[2], Sylvain Nicolay[5], Christophe Ballif[1,5], Ayodhya N. Tiwari[2] and Stephan Buecheler[2]

[1]Ecole Polytechnique Fédérale de Lausanne (EPFL), Institute of Microengineering (IMT), Photovoltaics and Thin-Film Electronics Laboratory (PV-Lab), Rue de la Maladière 71b, 2002 Neuchâtel, Switzerland

[2]Laboratory for Thin Films and Photovoltaics, Empa – Swiss Federal Laboratories for Materials Science and Technology, Ueberlandstrasse 129, CH-8600 Duebendorf, Switzerland

[3]Laboratory for Nanoscale Materials Science, Empa – Swiss Federal Laboratories for Materials Science and Technology, Ueberlandstrasse 129, CH-8600 Duebendorf, Switzerland

[4]Department of Physics, University of Basel, CH-4056 Basel, Switzerland

[5]CSEM, PV-Center, Jaquet-Droz 1, 2002 Neuchâtel, Switzerland

[6]Materials for Energy Conversion, Empa – Swiss Federal Laboratories for Materials Science and Technology, Ueberlandstrasse 129, CH-8600 Duebendorf, Switzerland

[*]E-mail: Fan.Fu@epfl.ch, Fan.Fu@empa.ch

Supplementary Table 1 | Summary of recently published long-term stability studies on perovskite solar cells.

	absorber	atmosphere	illumination	Temp. (°C)	Time (h)	comment
K.Bush et al.[1], Nat. Energy (2017)	$(Cs,FA)Pb(I,Br)_3$	Encapsulated, ambient air with 40% RH	Sulfur plasma lamp	35	1000	**No degradation**, but efficiency was not constant
S. Shin et al.[2], Science (2017)	$MAPbI_3$	Encapsulated; air	Xenon lamp	25	1000	Retained 93% of its initial efficiency
M. Saliba et al.[3], Science (2016)	$(RbCsFAMA)Pb(I,Br)_3$	Non-encapsulated; N_2	1-sun	85	500	Retained 95% of its initial efficiency
H. Tan et al[4]., Science (2017)	$(Cs,FA,MA)Pb(I,Br)_3$	Non-encapsulated; N_2	AM1.5G, 1-sun, 420-nm UV filter	25	500	Retained 95% of its initial efficiency
Aroara et al.[5], Science (2017)	$(Cs,FA,MA)Pb(I,Br)_3$	Non-encapsulated ; N_2	1-sun	60	1000	Retained 95% of its initial efficiency
Hou et al.[6], Science (2017)	$(FA,MA)Pb(I,Br)_3$	Non-encapsulated; N_2	1-sun	25	1000	Retained 95% of its initial efficiency

Supplementary Table 2 | Summary of photovoltaic parameters of $FAPbI_3$:MABr (10 mg ml^{-1}) perovskite solar cells presented in Figure 1d-e.

		V_{OC} (V)	J_{SC} (mA cm^{-2})	J_{SC} (mA cm^{-2}) from EQE	FF (%)	η (%)	η_{MPP} (%)	Cell area (cm^2)
initial	Forward	1.023	19.3	19.2	69.8	13.8	13.6	0.225
	Backward	1.062	19.8		69.1	14.5		
Prior 1000 hours @ 60 °C	Forward	1.044	18.3	19.1	62	11.8	12.7	0.25
	Backward	1.077	18.4		67.6	13.4		
After 320 hours @ 80 °C	Forward	1.131	7.1	19	56	4.5	4.7	0.225
	Backward	1.133	7.3		58	4.8		
After 320 hours @ 80 °C	Forward	1.131	18.2	19	56	11.5	12	0.088
	Backward	1.133	18.7		58	12.3		

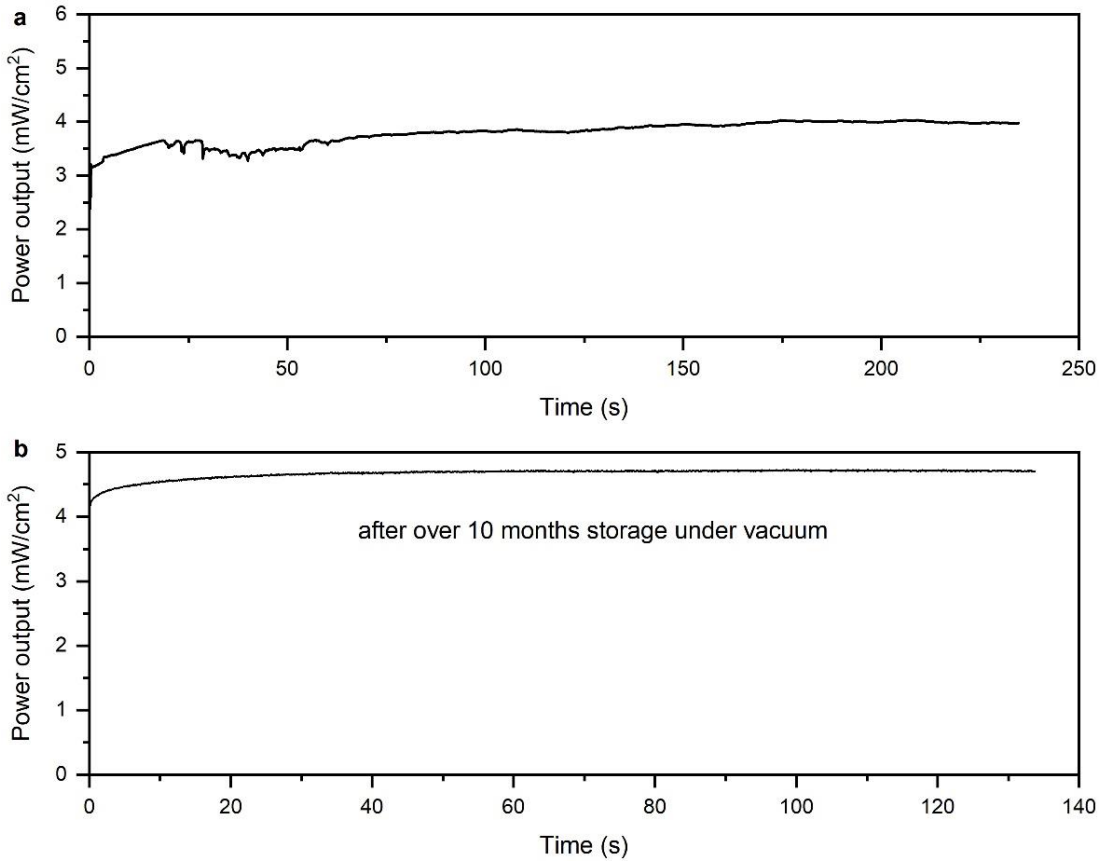

Supplementary Figure 1. Maximum power point (MPP) measurements of the cell after 320 h HLS at 80 °C. **a**, MPP measured after HLS. **b**, MPP measured after over 10 month storage in a vacuum chamber. The former measurement was performed at Empa and the later measurement was performed at EPFL-PV-Lab.

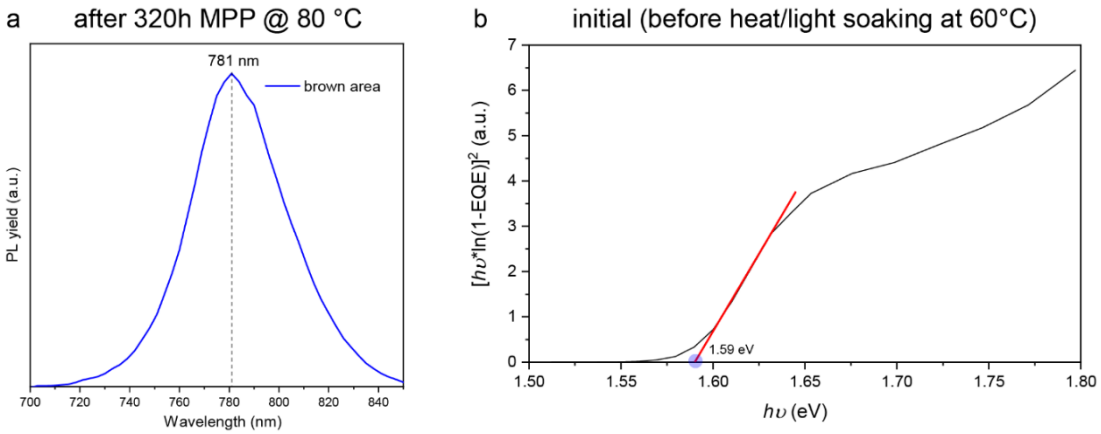

Supplementary Figure 2. **a**, Steady state photoluminescence (PL) spectrum taken in the remaining dark brown region. The PL peak position at 781 nm gives a bandgap of 1.59 eV. **b**, Tauc plot of the cell before any long-term heat light soaking test. A bandgap of 1.59 eV was extrapolated, which is in good agreement with the optical bandgap obtained from PL.

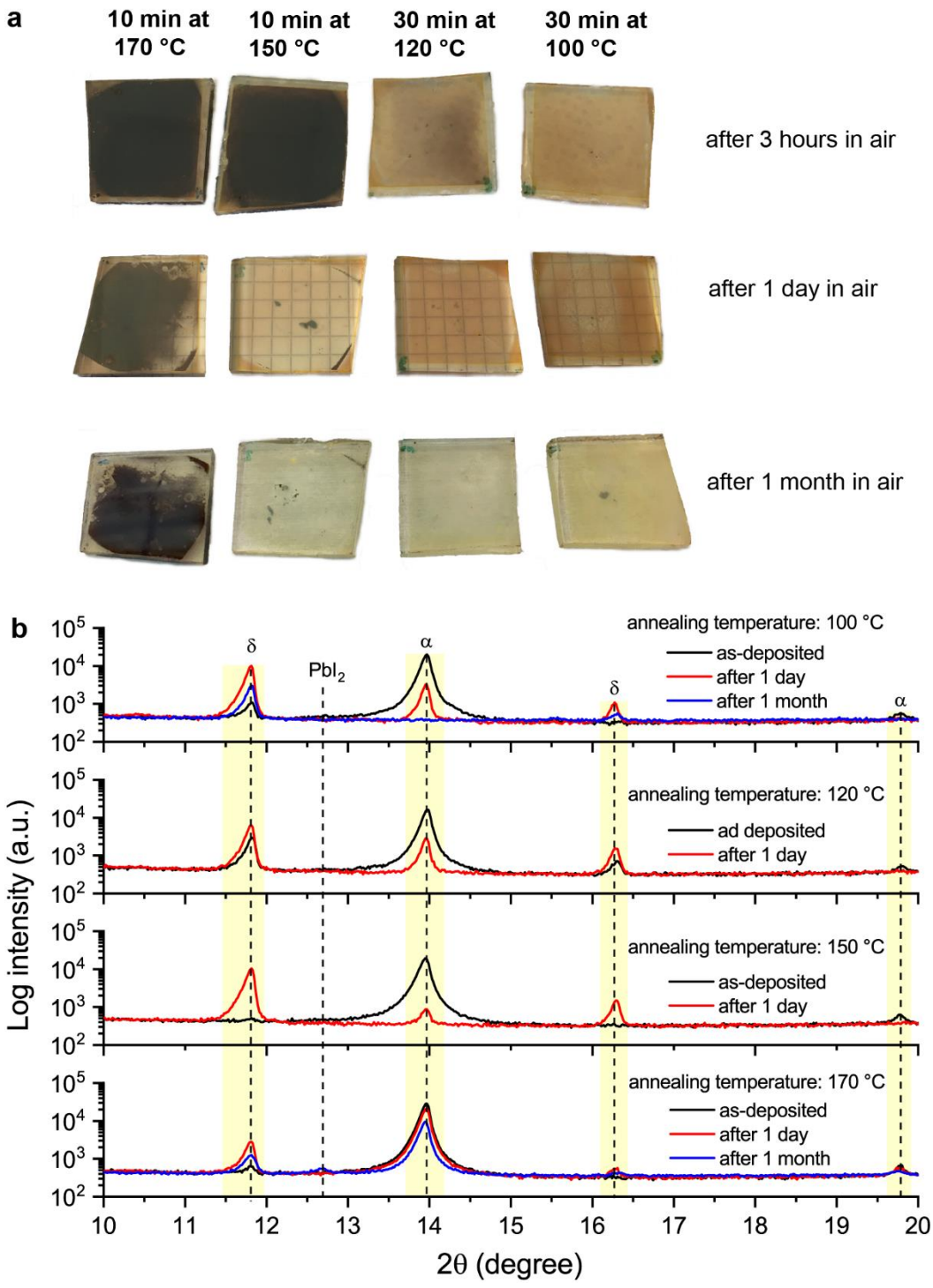

Supplementary Figure 3. Degradation behavior of α-$FAPbI_3$ absorbers in ambient air as a function of crystallization temperature. **a**, **b**, Photograph (**a**) and the corresponding XRD patterns (**b**) of α-$FAPbI_3$ layers after storage in ambient air for different periods of time.

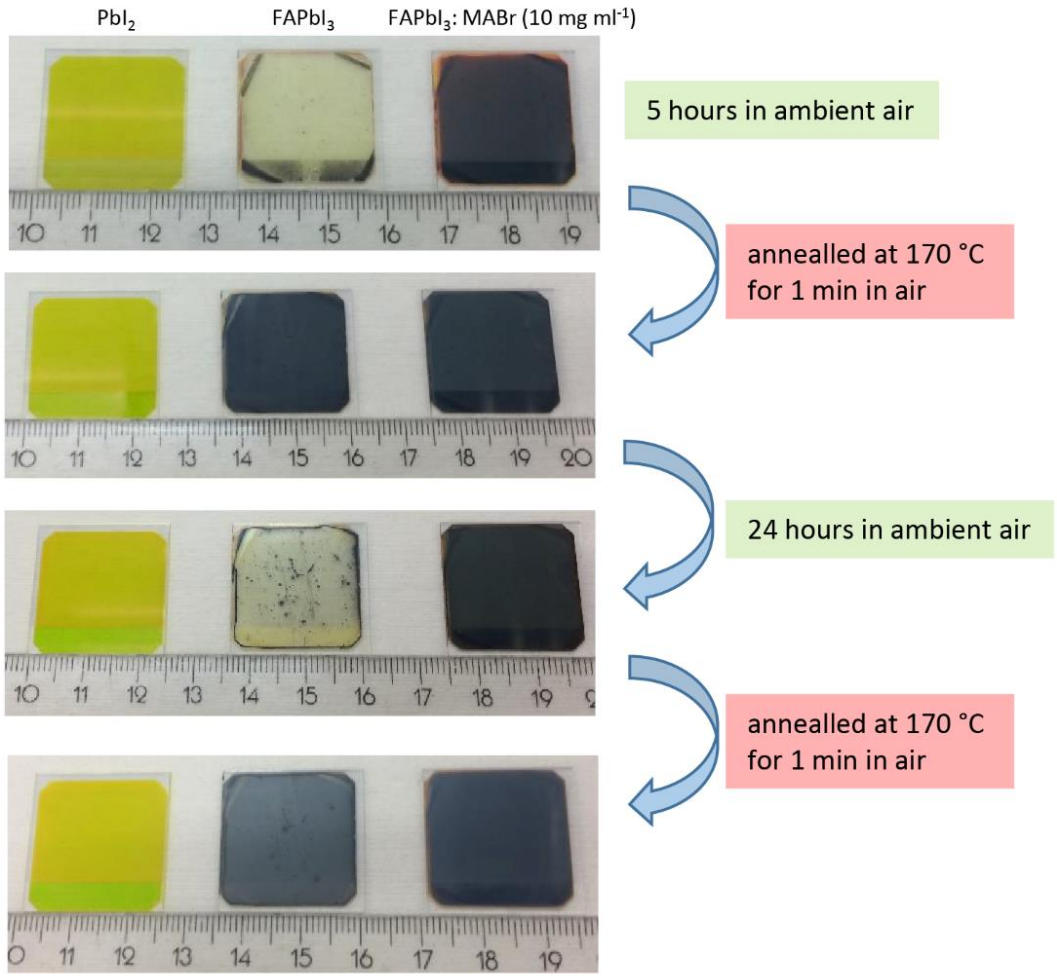

Supplementary Figure 4. Reversible conversion between α- and δ-$FAPbI_3$ perovskite layers. α-$FAPbI_3$ changed color rapidly upon exposure to air. The pale color indicates that the phase is not yellow phase PbI_2. When the degraded layer was placed on a hotplate at 170 °C for 1 min, the black α-$FAPbI_3$ phase formed again. This process is repeatedly reversible. Adding MA^+ and Br^- into α-$FAPbI_3$ enhances the air stability.

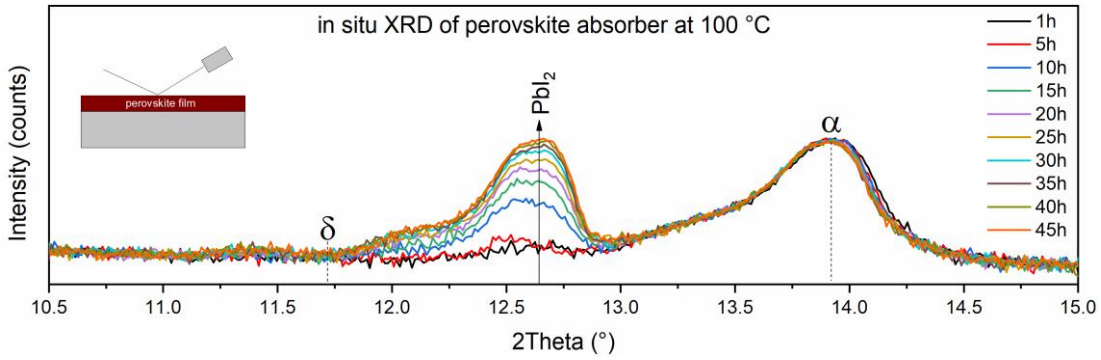

Supplementary Figure 5. In situ XRD of $FAPbI_3$:MABr (10 mg ml^{-1}) perovskite absorber measured at 100 °C. The sample was flushed with N_2 at a flow rate of 50 sccm. The perovskite phase degradation was much slower when the layer was directly exposed to the atmosphere compared to when it was included in a full device, suggesting the important role of trapped gas during the decomposition of the perovskite included in a full device.

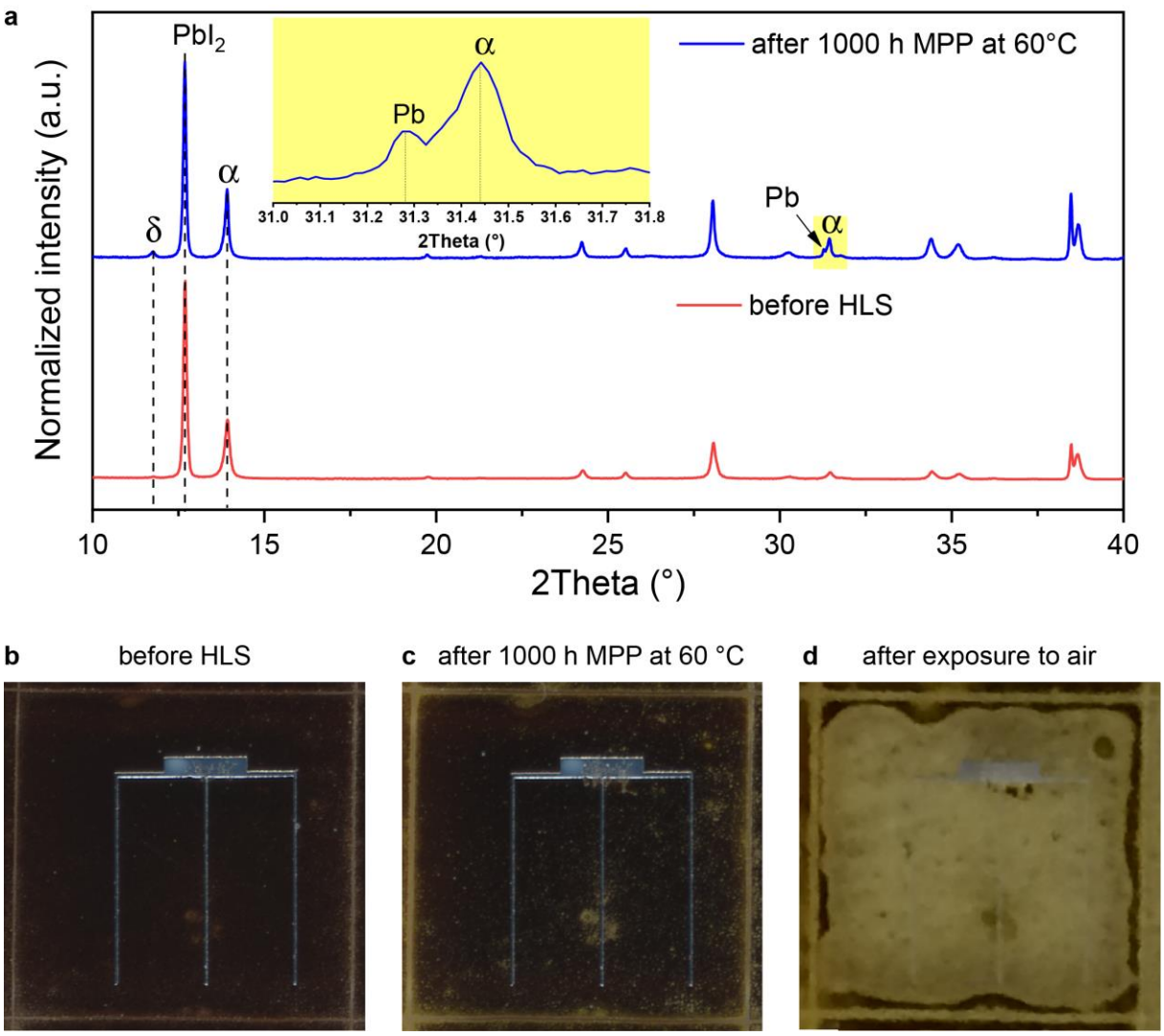

Supplementary Figure 6. **a**, XRD patterns of NIR-transparent solar cells featuring a $FAPbI_3$ absorber after 1000 hours MPP operation at 60 °C under 500 mbar N_2 atmosphere. In addition to a large PbI_2 peak, a small δ-$FAPbI_3$ reflection appeared and metallic Pb was detected after 1000 hours of HLS at 60 °C. **b**, **c**, **d**, photograph of the perovskite cell before HLS (**b**), after 1000 hours of MPP operation at 60 °C (**c**), and after exposure to ambient air (**d**). δ-$FAPbI_3$ and metallic Pb peaks were observed after 1000 hours of MPP operation at 60 °C.

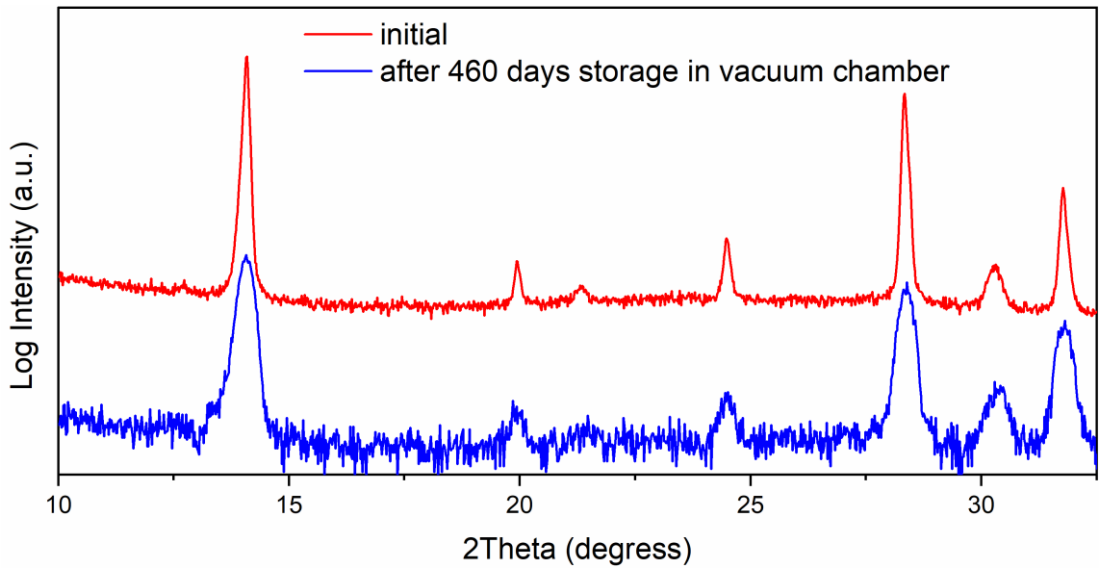

Supplementary Figure 7. X-ray diffraction patterns of α-$FAPbI_3$ perovskite after storage for over 460 days. The broadening of the peak is due to the fact that the XRD was performed on an apparatus with lower resolution.

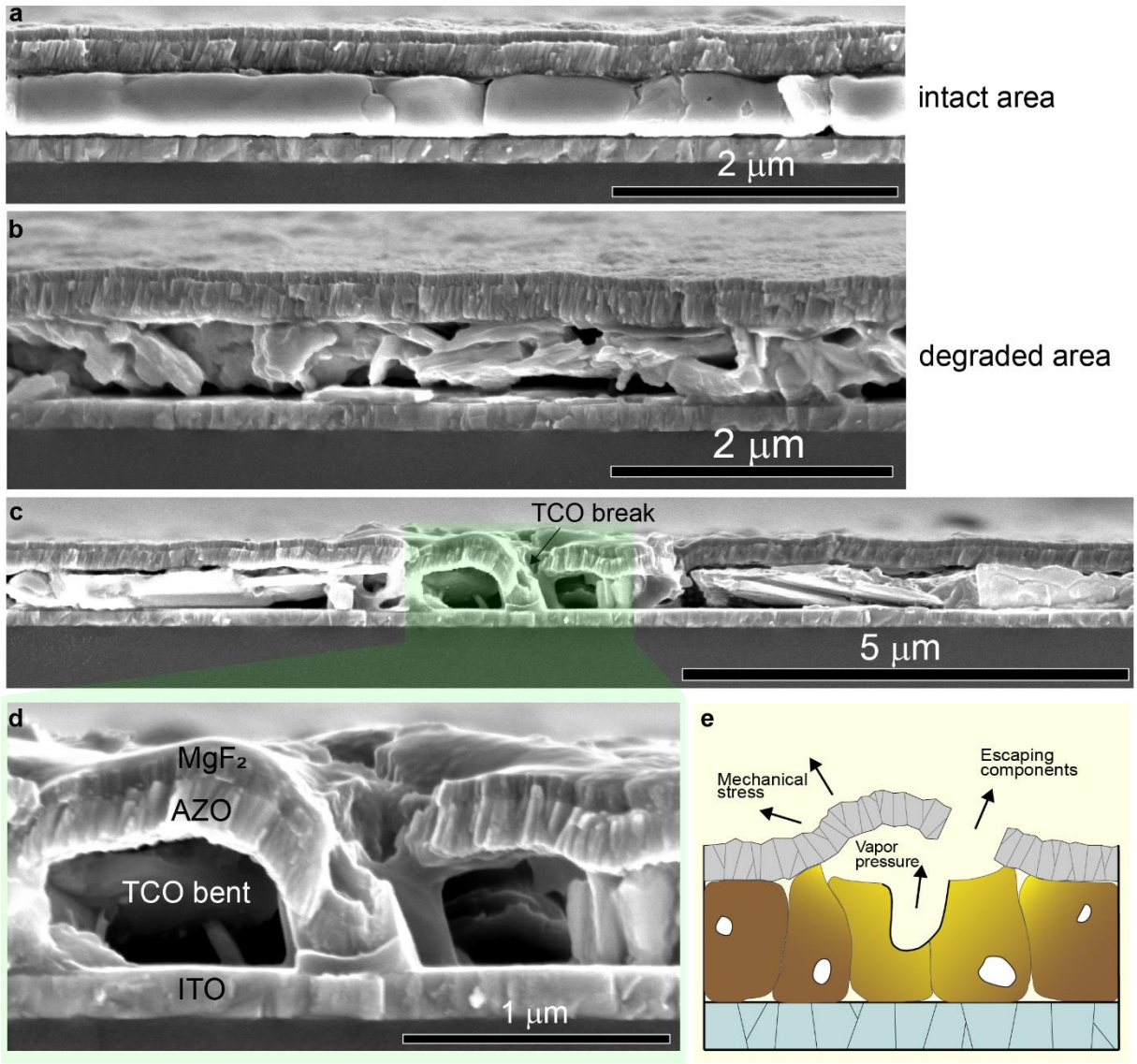

Supplementary Figure 8. Cross-sectional SEM images of NIR-transparent perovskite solar cell after in situ XRD at 100 °C. **a**, **b**, Intact (**a**) and degraded areas (**b**). **c**, Degraded area with a ruptured TCO. **d**, Zoom in the area that shows an opened top electrode. **e**, Schematic illustration of the process occurring due to a pressure of volatile components building up as a result of the degradation of the perovskite absorber.

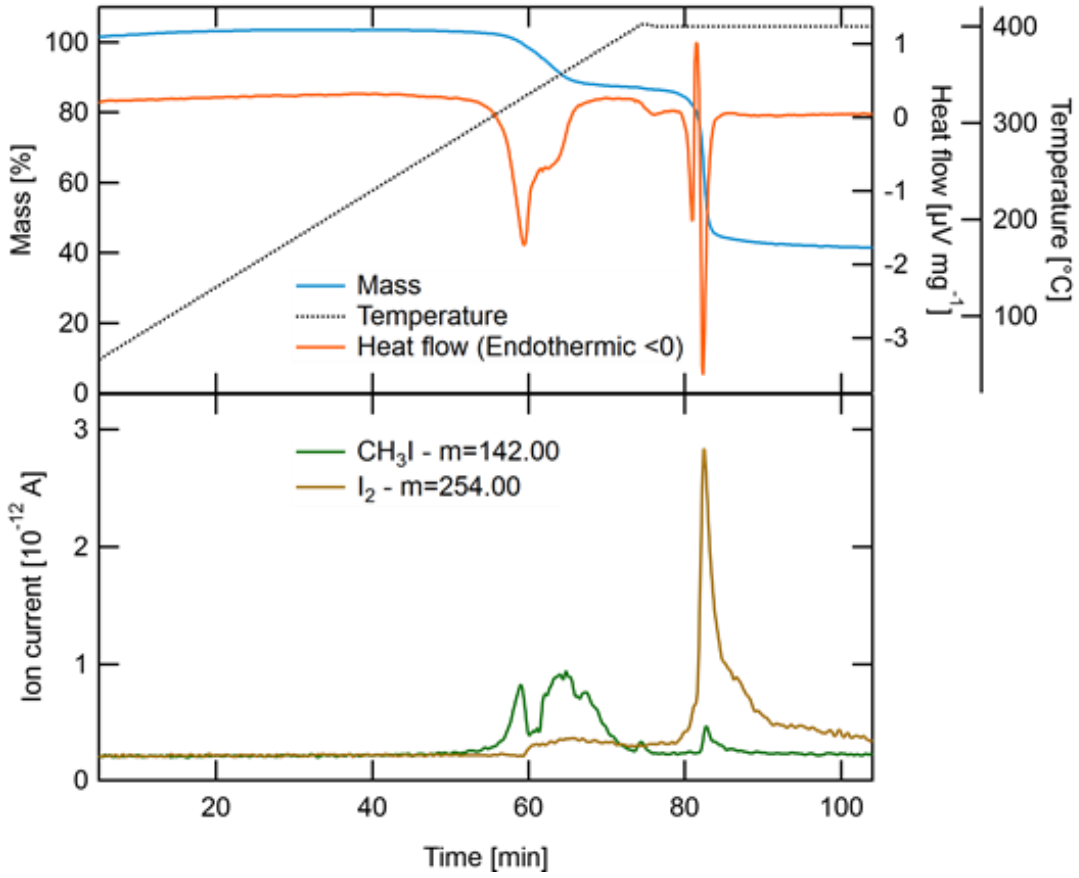

Supplementary Figure 9. Thermogravimetric analysis/mass spectroscopy (TGA-MS) measurement of $FAPbI_3$:MABr (10 mg ml^{-1}) powder up to 400 °C. I_2 vapor is one of the main gas product after perovskite decomposition.

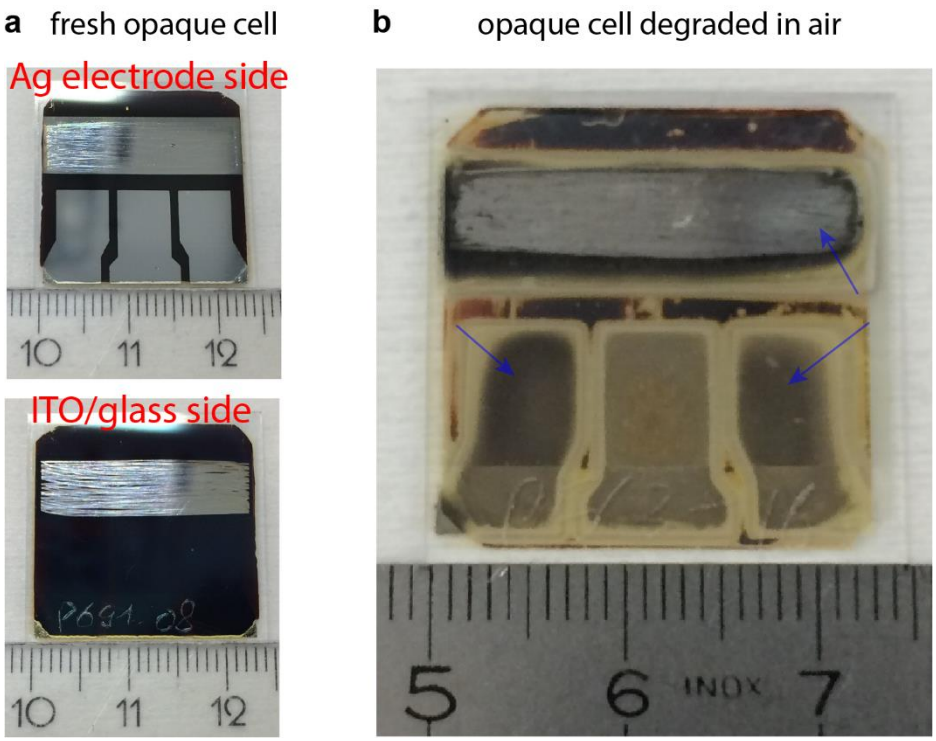

Supplementary Figure 10. Degradation behavior of opaque cells stored in ambient air. **a**, Photographs of a typical non-degraded opaque perovskite solar cell viewed from the Ag electrode side and the ITO/glass side, respectively. **b**, Photographs of an opaque sample degraded in ambient air. The degradation of the perovskite solar cell initiated from the cell edges and propagated towards the cell center as indicated by the blue arrows.

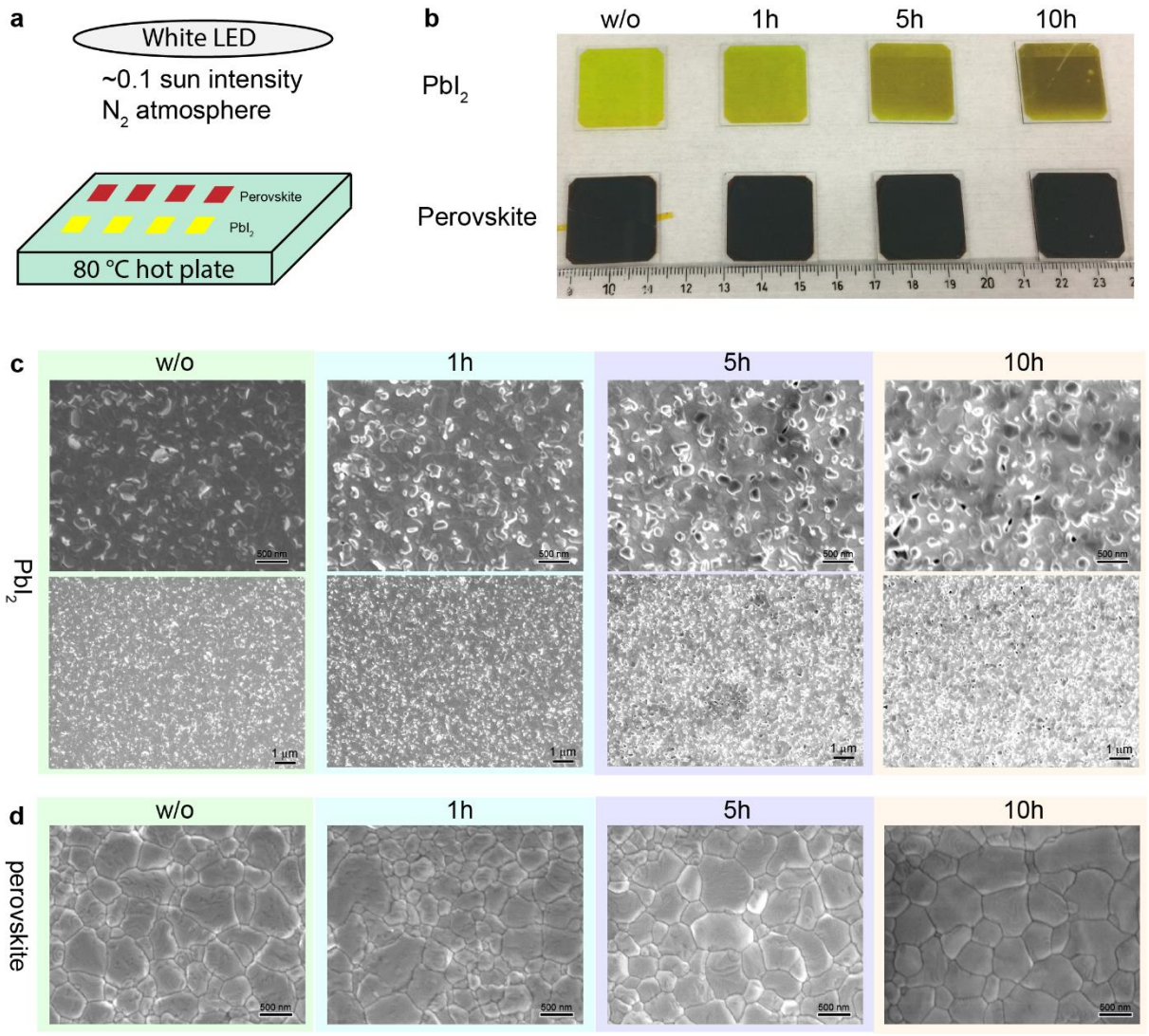

Supplementary Figure 11. Heat-light soaking (HLS) of perovskite and PbI_2 films. **a**, Schematic illustration of the HLS experiments. **b**, Photographs of PbI_2 and perovskite films after various periods of HLS. **c**, **d**, Cross-sectional SEM images of PbI_2 (**c**) and perovskite (**d**) films subjected to various periods of HLS. The perovskite ($FAPbI_3$:MABr (10 mg ml^{-1})) and PbI_2 films were placed on a 80 °C hotplate under a ~0.1 sun illumination using a white LED array. The experiments were performed inside a N_2-filled glovebox to minimize the influence of H_2O and O_2 (H_2O and O_2 < 0.1ppm).

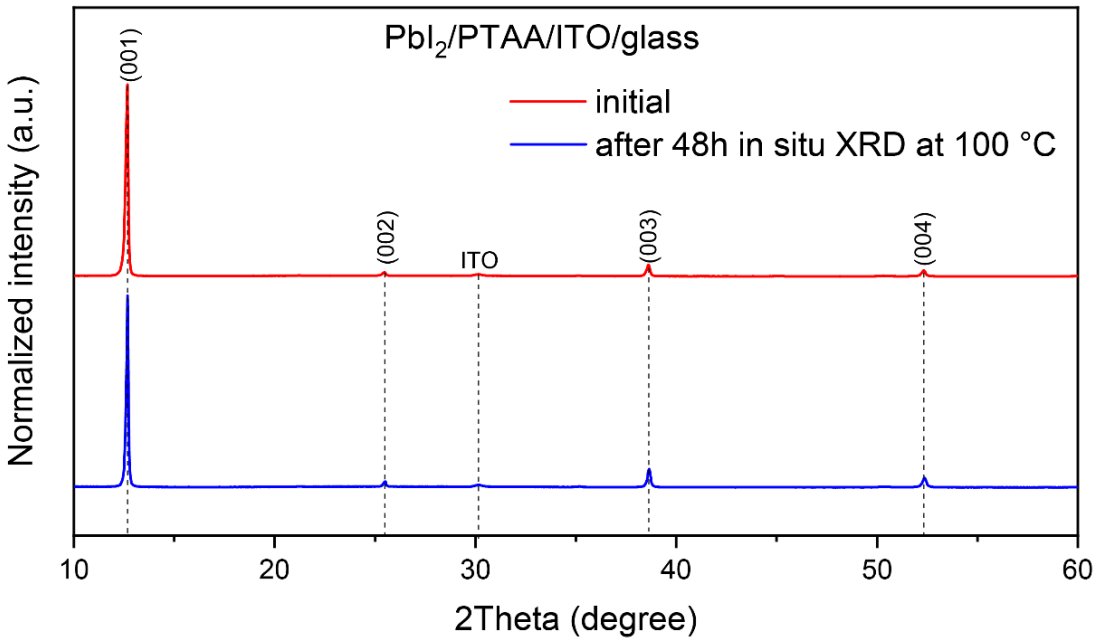

Supplementary Figure 12. X-ray diffraction patterns of a PbI_2 layer heated at 100 °C for 48 hour in the dark. No metallic Pb peak was detected after 48 hours of measurement at 100 °C.

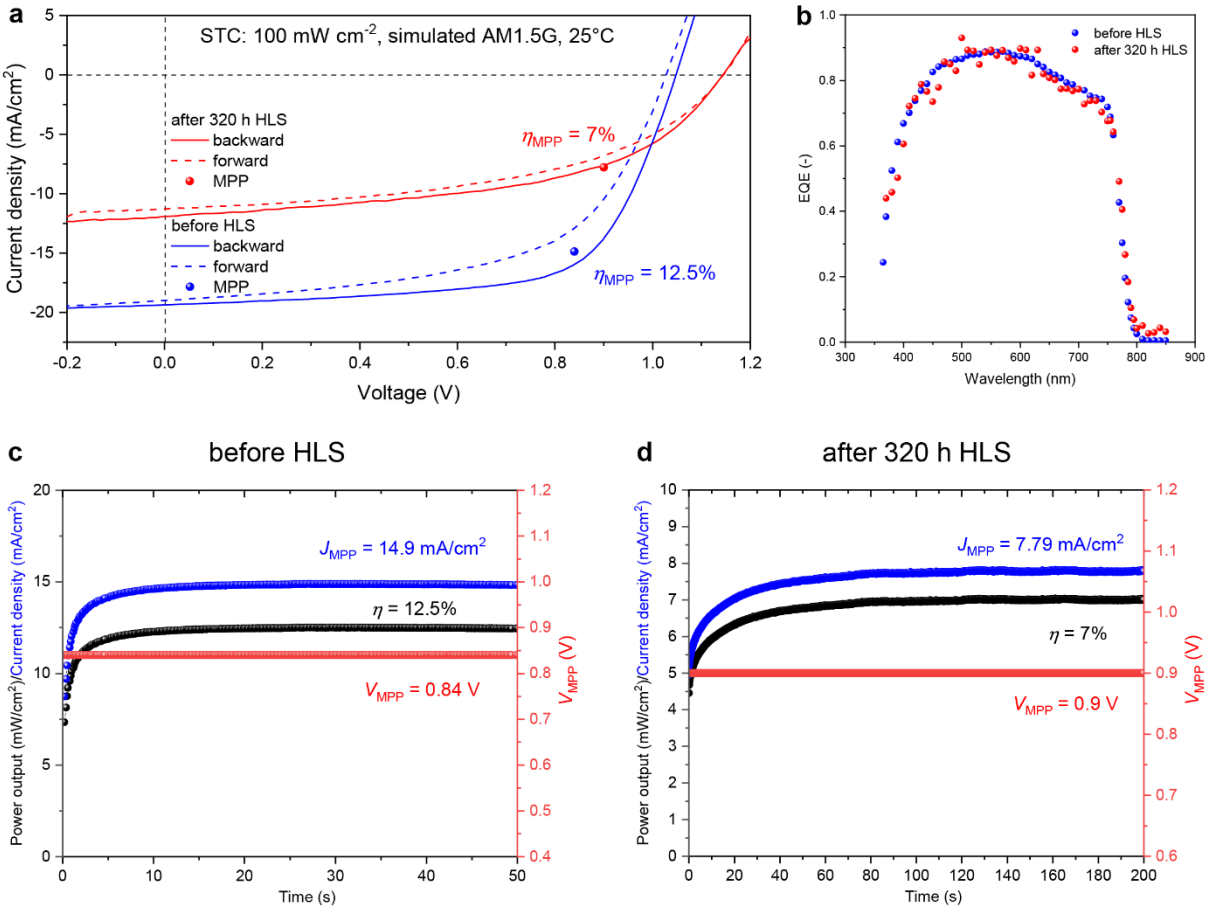

Supplementary Figure 13. Photovoltaic performance of a NIR-transparent $FAPbI_3$:MABr (20 mg ml^{-1}) solar cell. **a**, **b**, The *J-V* curves (**a**) and EQE spectra (**b**) of the sample measured before and after HLS (320 hours MPP operation under equivalent 1-sun illumination at 80 °C under N_2 atmosphere). **c**, **d**, The MPP measurements of the perovskite cell before (**c**) and after (**d**) HLS under STC. The *J-V* curves and MPP measurements before and after HLS were measured at Empa and EPFL, respectively.

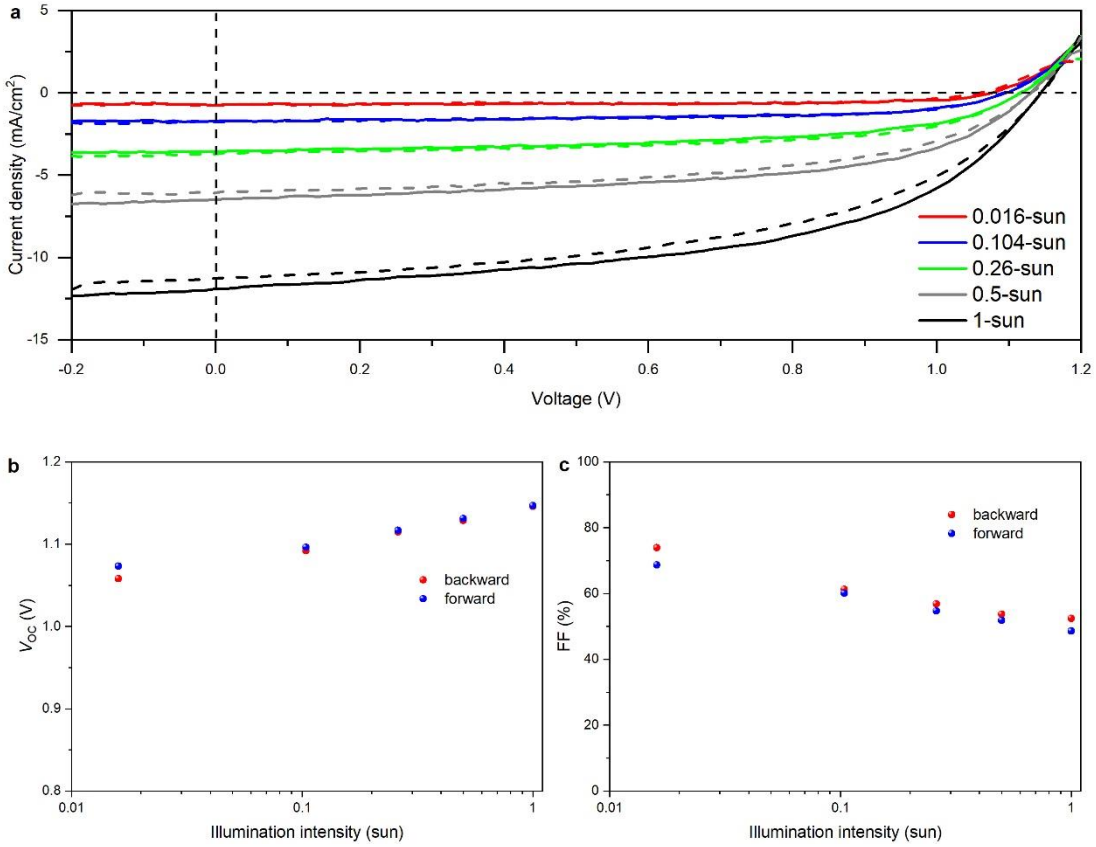

Supplementary Figure 14. Illumination intensity-dependent photovoltaic performance of NIR-transparent $FAPbI_3$:MABr (20 mg ml^{-1}) solar cell after HLS. **a**, *J-V* curves measured at various illumination intensities of a simulated AM1.5G solar spectrum. **b**, **c**, Illumination intensity-dependent V_{OC} (**b**) and FF (**c**). The V_{OC} remains larger than 1.05 V and the FF approaches 75% under a low illumination intensity of 0.016 sun.

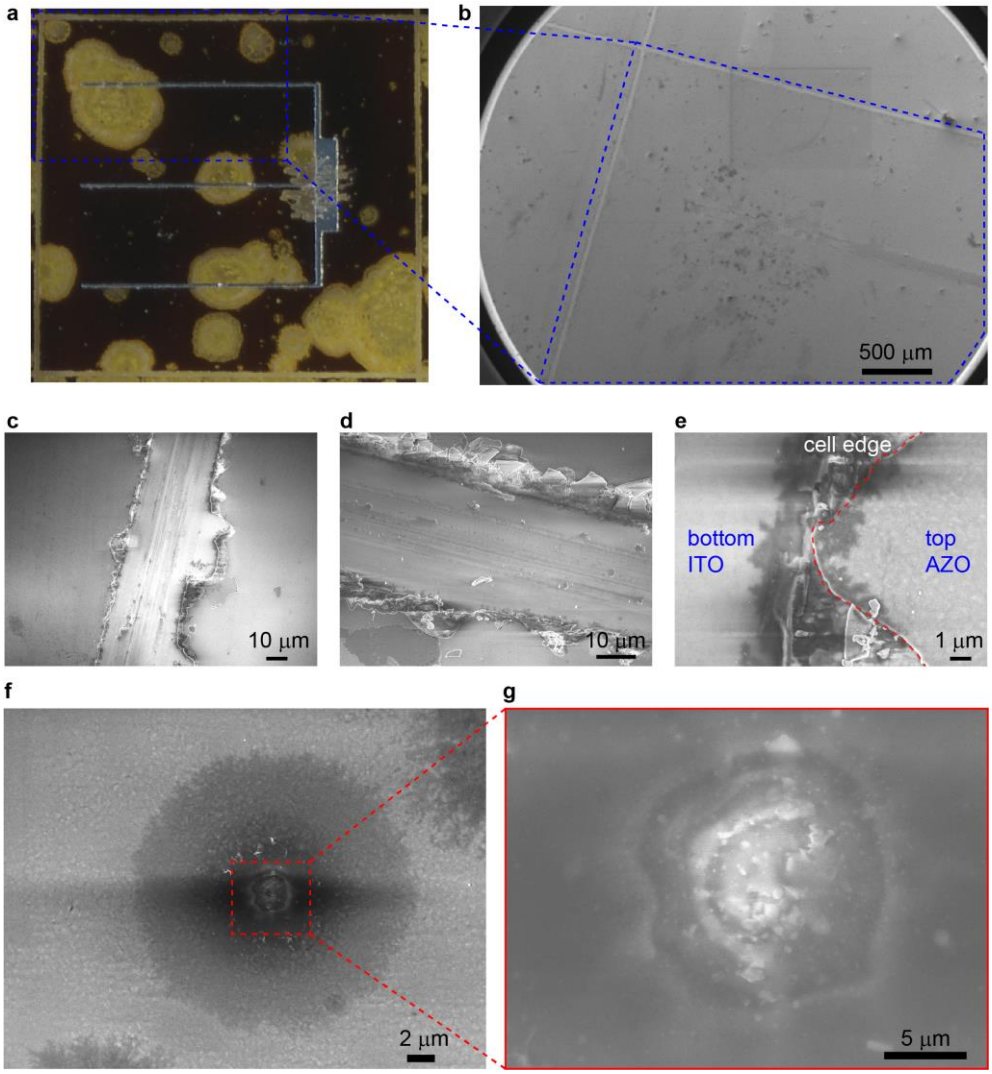

Supplementary Figure 15. Top-view SEM images of $FAPbI_3$:MABr (20 mg ml^{-1}) solar cells. **a**, Photograph of the cell after 320 hours of MPP operation at 80 °C under 1-sun illumination and 500 mbar N_2 atmosphere. **b**, Low-magnification top-view SEM image. **c**, **d**, **e**, Top-view SEM images of scribe line at cell edge. f, g, High-magnification top-view SEM images on a degradation center.

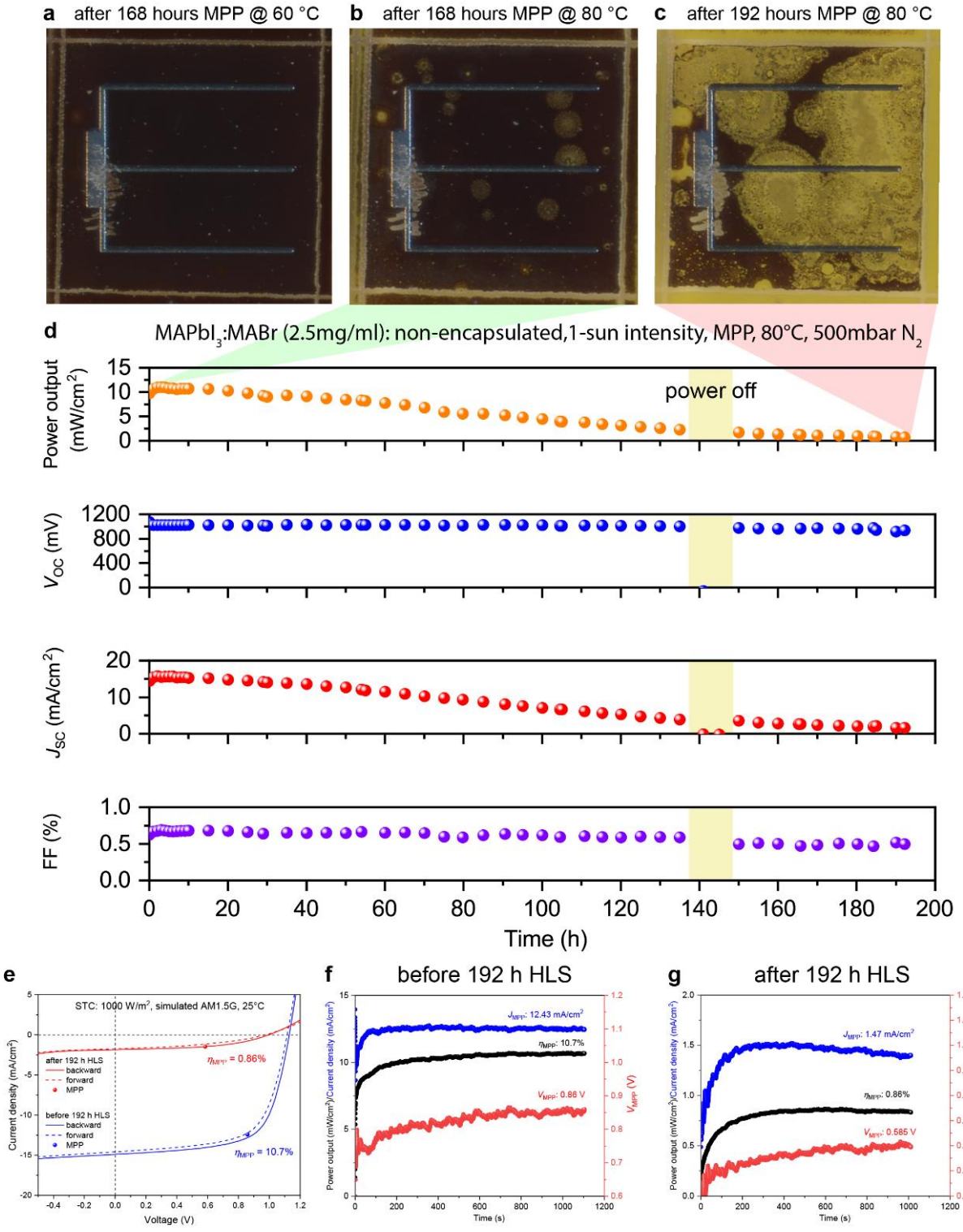

Supplementary Figure 16. Operational stability of $MAPbI_3$:MABr (2.5 mg ml^{-1}) solar cells at 80 °C under 500 mbar N_2 atmosphere. **a**, **b**, **c**, Photograph of the cell after different stressing conditions. **d**, The photovoltaic parameters of the cell stressed at 80 °C for 192 hours. **e**, *J-V* curves of the cell measured before and after 192 h HLS under STC. **f**, **g**, MPP measurements before (**f**) and after (**g**) 192 h HLS under STC.

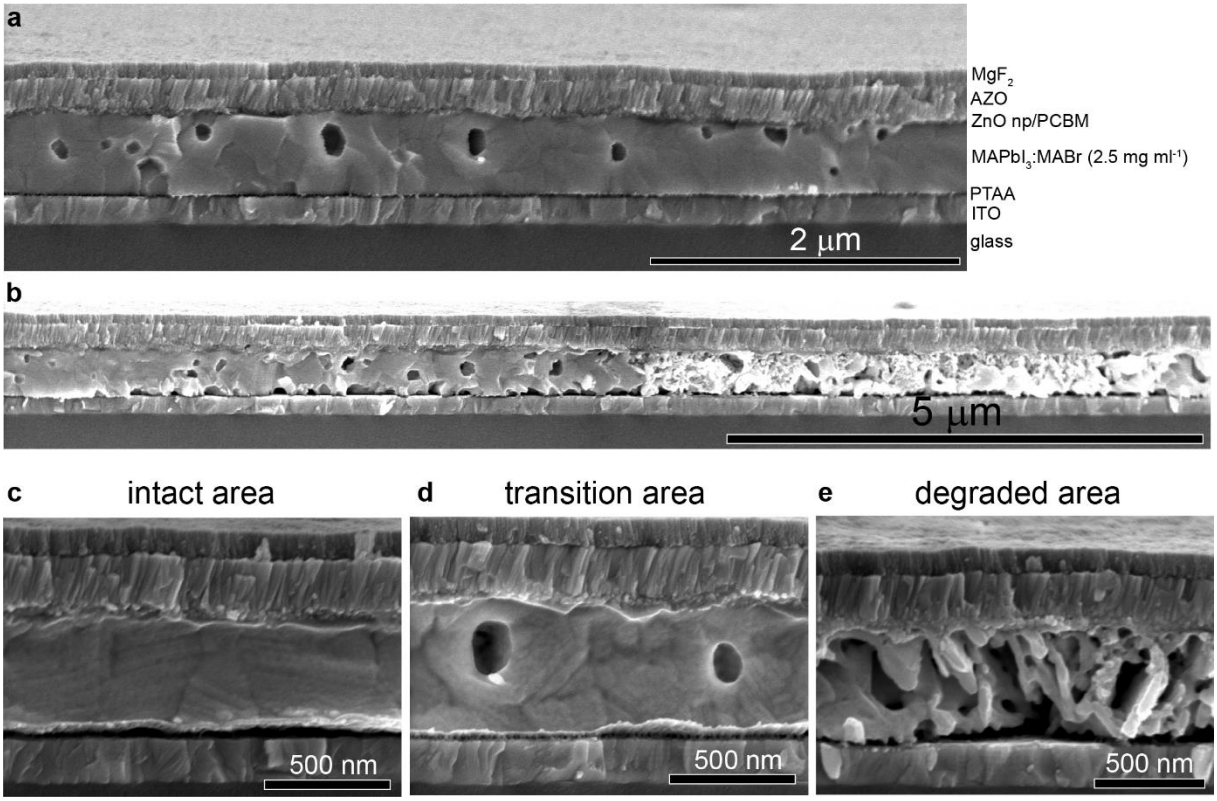

Supplementary Figure 17. Cross-sectional SEM images of NIR-transparent $MAPbI_3$:MABr (2.5 mg ml^{-1}) solar cell after 192 h HLS (MPP operation under 1-sun illumination at 80 °C under 500 mbar N_2 atmosphere). **a**, The typical transition area of the cell shows plenty of holes inside the perovskite absorber. **b**, SEM image spanning across transition area and degraded area. **c**, **d**, **e**, High magnification images of the intact (**c**), transition (**d**), and degraded areas (**e**) of the perovskite cell. The $MAPbI_3$-based cell shows a similar degradation behavior as $FAPbI_3$-based devices, suggesting a similar microscopic degradation mechanism.

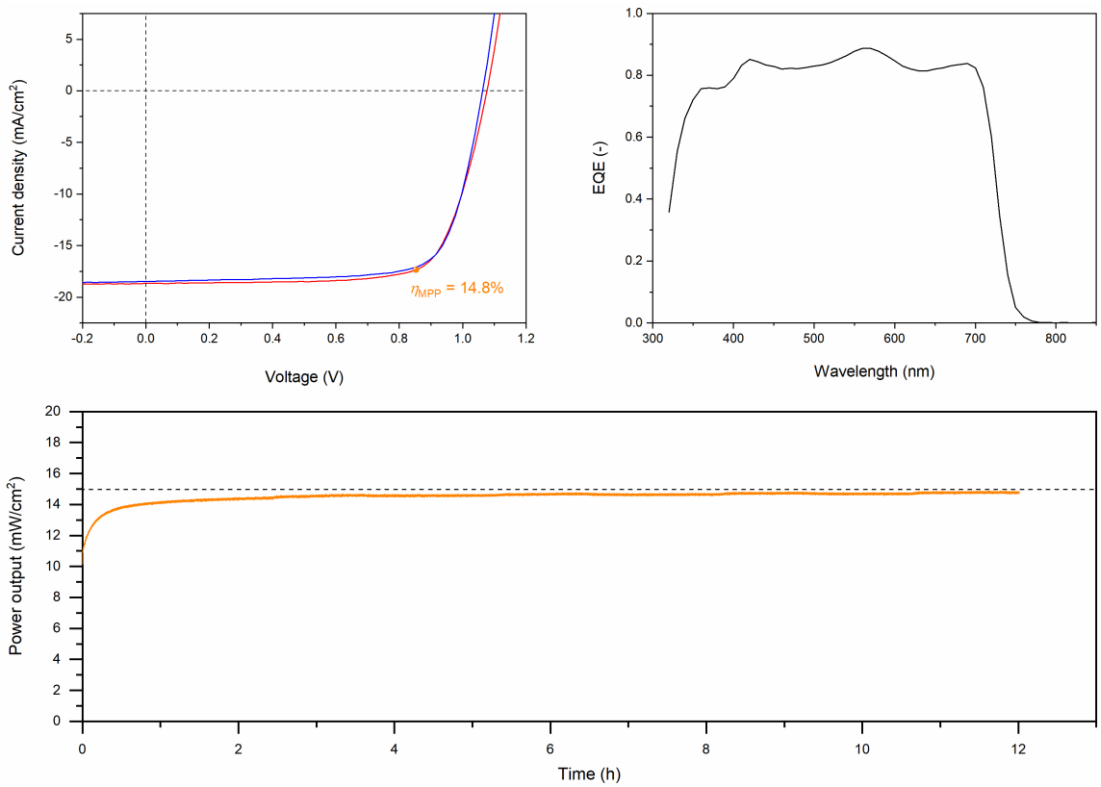

Supplementary Figure 18. Photovoltaic performance of an opaque perovskite cell with a 1.7 eV bandgap. **a**, **b**, **c**, *J*-*V* curve (**a**), EQE (**b**), and overnight MPP measurement (**c**). The device structure is glass/ITO/PTAA/(Cs,FA)Pb(I,Br)$_3$ perovskite absorber/C60/TmPyPb/Ag and cell area is 0.25 cm^2 defined by a metal mask. No active cooling is applied during MPP measurement and the temperature increase to above 40 °C. The relative humidity is around 40% during measurement.

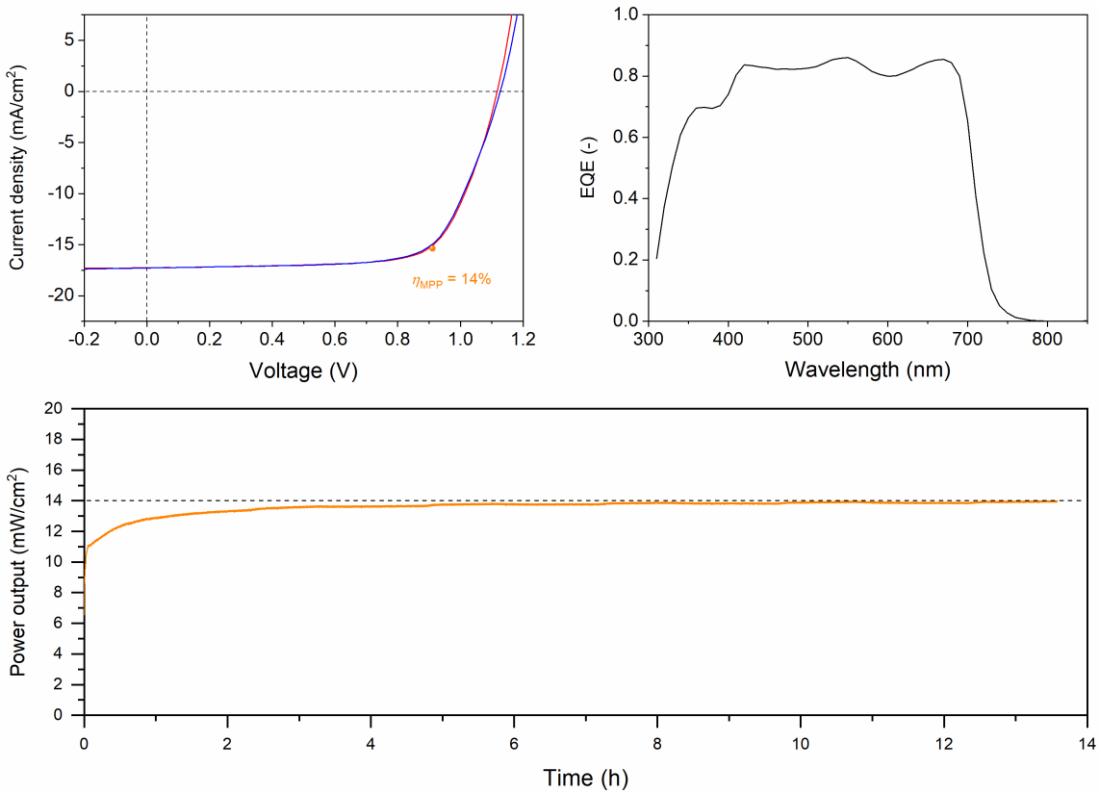

Supplementary Figure 19. Photovoltaic performance of an opaque perovskite cell with a 1.75 eV bandgap. **a**, **b**, **c**, *J*-*V* curve (**a**), EQE (**b**), and overnight MPP measurement (**c**). The device structure is glass/ITO/PTAA/(Cs,FA)Pb(I,Br)$_3$ perovskite absorber/C60/TmPyPb/Ag and cell area is 0.25 cm^2 defined by a metal mask. No active cooling is applied during MPP measurement and the temperature increase to above 40 °C. The relative humidity is around 40% during measurement.

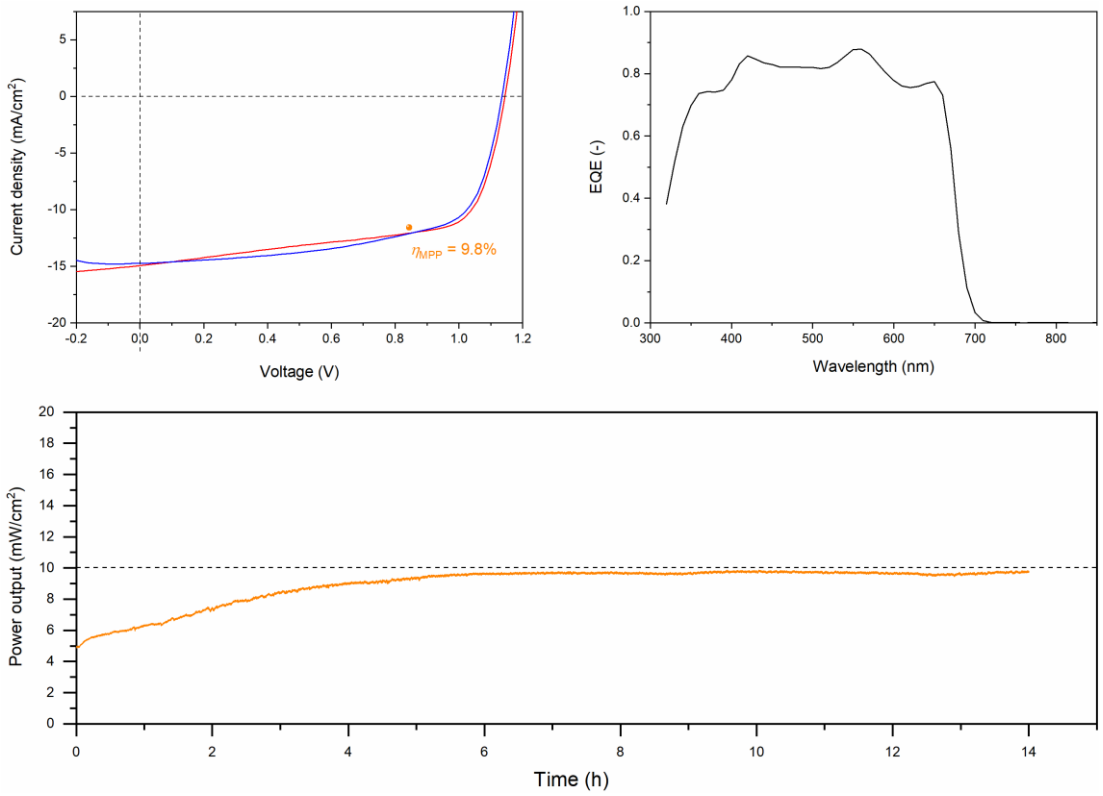

Supplementary Figure 20. Photovoltaic performance of a perovskite cell with a 1.82 eV bandgap. **a**, **b**, **c**, *J-V* curve (**a**), EQE spectrum (**b**), and overnight MPP measurement (**c**). The device structure is glass/ITO/PTAA/(Cs,FA)Pb(I,Br)$_3$ perovskite absorber/C60/TmPyPb/Ag and cell area is 0.25 cm^2 defined by a metal mask. No active cooling is applied during MPP measurement and the temperature increase to above 40 °C. The relative humidity is around 40% during measurement.

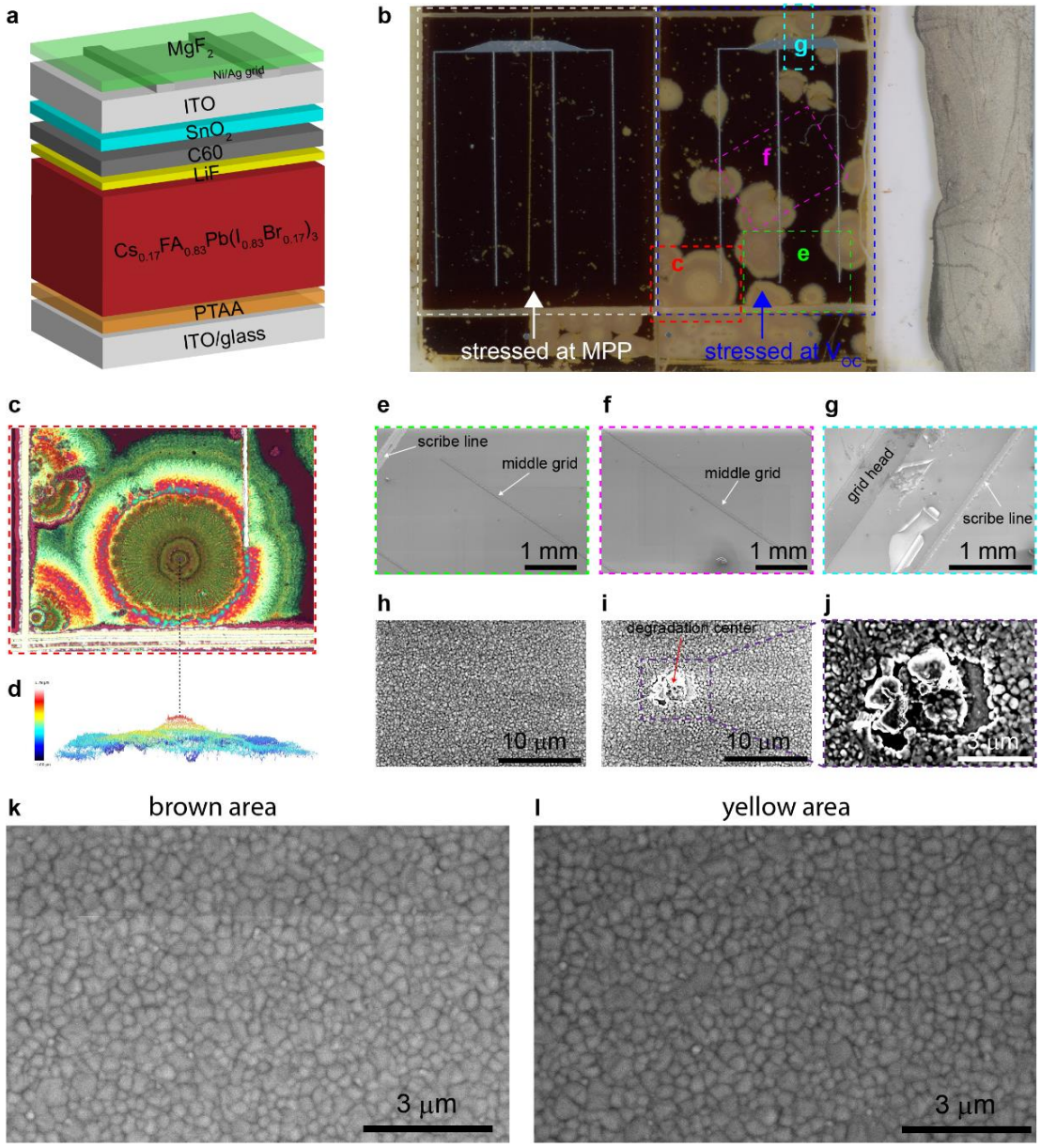

Supplementary Figure 21. **a**, Schematic device structure of $Cs_{0.17}FA_{0.83}Pb(I_{0.83}Br_{0.17})_3$ perovskite solar cell. **b**, Photograph of two cells after 1000 hours HLS at 80 °C under 1-sun illumination and 500 mbar atmosphere. **c, d,** 3D optical microscopy image (**c**) and corresponding height profile (**d**) taken at region marked in **Supplementary Figure 21b**. **e, f, g,** Top view SEM image took at regions marked in **Supplementary Figure 21b**. **h**, Top-view SEM image close to a degradation center. **i**, Top-view SEM image of a degradation center. **j**, Zoom in morphology of the degradation center. **k, l,** Top-view SEM images of area taken at brown (**k**) and yellow (**l**) area. There is no difference between SEM images taken at brown and yellow region because what we observe is actually the morphology of top MgF_2 layer.

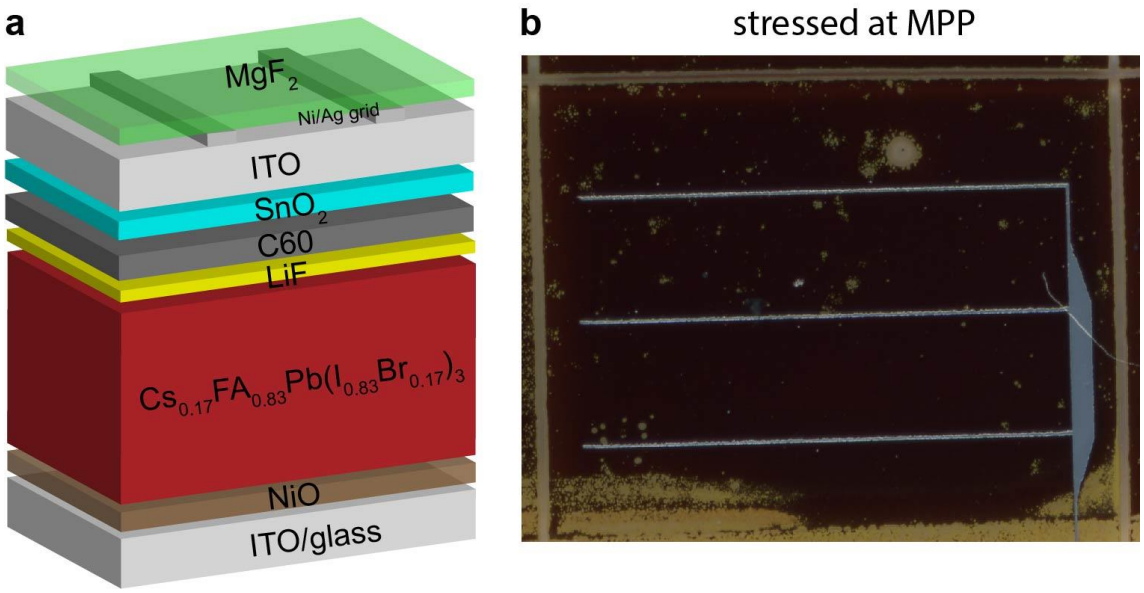

Supplementary Figure 22. **a**, Schematic device structure of $Cs_{0.17}FA_{0.83}Pb(I_{0.83}Br_{0.17})_3$ perovskite solar cell with NiO hole transport layer. **b**, Photograph of two cells after 1000 hours of MPP at 80 °C under 1-sun illumination and 500 mbar atmosphere.

1. Bush, K. A. *et al.* 23.6%-efficient monolithic perovskite/silicon tandem solar cells with improved stability. *Nat. Energy* **2**, 17009 (2017).
2. Shin, S. S. *et al.* Colloidally prepared La-doped BaSnO₃ electrodes for efficient, photostable perovskite solar cells. *Science (80-.).* **356**, 167 LP – 171 (2017).
3. Saliba, M. *et al.* Incorporation of rubidium cations into perovskite solar cells improves photovoltaic performance. *Science (80-.).* **354**, 206–209 (2016).
4. Tan, H. *et al.* Efficient and stable solution-processed planar perovskite solar cells via contact passivation. *Science (80-.).* **355**, 722 LP – 726 (2017).
5. Arora, N. *et al.* Perovskite solar cells with CuSCN hole extraction layers yield stabilized efficiencies greater than 20%. *Science (80-.).* **358**, 768 LP – 771 (2017).
6. Hou, Y. *et al.* A generic interface to reduce the efficiency-stability-cost gap of perovskite solar cells. *Science (80-.).* **5561**, eaao5561 (2017).